Friction

Research Article

Electrically promoted tribological changes at diamond-like carbon/steel interface under lubrication conditions

Fu Wang[1,✉], Yihua Wang[2], Xinjian Dong[1], Zhibo Wang[1], Dongshan Li[1], Guangan Zhang[1,✉]

Cite this article: Wang F, Wang YH, Dong XJ, et al. *Friction* 2026, **14**(1): 9441088. https://doi.org/10.26599/FRICT.2025.9441088

ABSTRACT: In modern machinery, electrified contacts present novel lubrication challenges for sliding components. Understanding the electrified tribological characteristics of tribomaterials is vital. This work studied the electrified tribological changes at a diamond-like carbon (DLC)/steel sliding interface when lubricated with base oils. The results showed that electric current induced sticking friction, resulting in a friction reduction of approximately 5%–20% when mineral, PAO6, and castor oils were used in short-duration tests; conversely, there was a slight increase in friction with rapeseed oil. The electric current triggered the growth of a graphite-like tribo-layer on the DLC surface, particularly at the ester-lubricated interfaces, which mitigated the wear of the DLC. As sliding progressed, the DLC film experienced peeling wear under electrified conditions, especially at high currents and loads. The tribo-layer, formed from tribo-oxidation of the steel pair and lubricant degradation, was correlated with electrified tribological behavior. The enhanced adhesive and molecular interactions caused by the electric field across the contact were deemed to contribute to friction under electrified conditions. These findings validate the electrically caused tribological changes in lubricated DLC/steel contacts and indicate the necessity of a novel DLC film design to counteract electrified-induced damage.

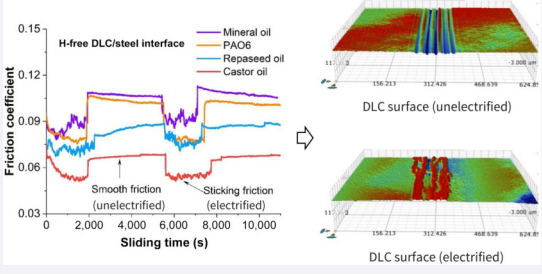

KEYWORDS: diamond-like carbon (DLC) film; electrified contact; lubrication; friction; wear

1 Introduction

Friction and wear are crucial topics for moving contact systems and have a major impact on the reliability and longevity of mechanical parts. With the advent of several new industries, such as electric vehicles, electrified railroads, industrial generators, and electromagnetic rail guns, tribology has increasingly focused on the electrified friction and wear properties of materials in recent years [1, 2]. Conductive materials, such as gold, silver, copper, and carbon, have been examined under current-carrying situations to ensure power transmission and lubrication of electrical contact parts [3–7]. It is widely acknowledged that Joule heating and arc effects, coupled with mechanical stress and frictional heat, significantly modify the friction and wear characteristics of electrified contacts [1, 2, 8]. Therefore, it is essential to study the electrified tribological properties of self-lubricating and wear-resistant materials to meet the lubrication requirements of advanced electrical contact systems.

Diamond-like carbon (DLC) films are famous for their high hardness, low friction coefficient, exceptional wear resistance, and adjustable electrical properties. These attributes have led to their widespread application in surface protection for mechanical components, including automobile parts, bearings, gears, and tools [9–11]. Many factors influence the tribological properties of DLC films, including the structure and composition of the films, surface morphology, contact conditions, and environment [12–17]. With a focus on specific applications, the friction and wear properties of DLC films are examined under a variety of conditions [18–22]. As candidate tribological coatings for electrified components, the electrified tribological properties of DLC films have been studied by various research communities.

Wang et al. [23] studied the electrified friction and wear properties of metal-doped DLC films under dry conditions. The DLC films exhibited greater wear under current-carrying conditions. Ti doping harms the electrified friction of the DLC film. Sun and Diao [3] reported that increasing the current density across a contact decreased the friction coefficient of an amorphous carbon film from 0.20 to 0.03. The graphene nanosheets formed at the sliding interface dominated the electrified friction behavior. In a carbon-coated ball bearing, notable friction reduction and carbon film wear alleviation were reported when currents were applied [24]. Wang et al. [25] revealed that the oxidation of the steel counterpart is related to the electrified friction and wear behavior of the DLC film in unlubricated contact. Farfan-Cabrera et al. [26] reported, under mineral oil lubrication conditions, that the electric current-induced friction and wear increased for

[1] State Key Laboratory of Solid Lubrication, Lanzhou Institute of Chemical Physics, Chinese Academy of Sciences, Lanzhou 730000, China. [2] School of Chemical Engineering, Lanzhou University of Arts and Science, Lanzhou 730000, China.

✉ Corresponding authors. E-mail: F. Wang, fuwang@licp.cas.cn; G. Zhang, gazhang@licp.cas.cn

Received: September 26, 2024; Revised: January 19, 2025; Accepted: February 27, 2025

tetrahedrally bonded H-free DLC films but had a negligible influence on HDLC films. Ding et al. [27] reported that the liner bulges on the DLC surface in electrified contact lubricated with poly-α-olefin oil. A graphitization mechanism has been proposed to explain the electrified tribological behavior of DLC films [26, 27]. Braceras et al. [28] noted that contact resistance is a good monitoring tool for the status of DLC coatings. Overall, different tribological characteristics have been observed for DLC films in electrified contacts. However, owing to the extreme flexibility in the structure and chemistry of DLC films, as well as their diverse operating conditions, the electrified tribological behavior of DLC films has not been adequately explored.

In this work, we investigated the electrified tribological properties of H-free DLC films with a Cr adhesion interlayer prepared via magnetron sputtering in lubricated contact configurations utilizing steel balls as the counterpart. The lubricants employed in this research included two important biobased ester oils and two prevalent hydrocarbon-based oils. The electrified tribological characteristics of the system were examined under various conditions. A detailed analysis was performed on both friction surfaces to gain insights into the electrified friction and wear behaviors. The electrically promoted tribological changes on the DLC and steel surfaces were scrutinized to understand the electrified friction and wear properties. Our findings revealed that the localized DLC film peeling, lubricant degradation, tribo-oxidation, and electric field across the contact collectively affected the electrified tribological properties of the DLC films.

2 Materials and methods

2.1 Materials

Polyalphaolefin (PAO6), a synthetic chain hydrocarbon oil, was obtained from Beijing Xirunte Trading Co., Ltd., China. Hydrogenated refined mineral base oil(III) containing chain hydrocarbons and naphthene was obtained from Shenzhen Zhongruntong Chemical Co., Ltd., China. Two biobased ester oils, rapeseed and castor oils, with carbon–carbon double bonds and hydroxyl functional groups on their fatty acid chains, respectively, were purchased from Shanghai Aladdin Biochemical Technology Co., Ltd., China. Table 1 shows the kinematic viscosity of the above four base oils at 100 °C.

2.2 Film preparation

The DLC film was prepared on bearing steel substrates via a closed-field unbalanced magnetron sputtering coating system (Teer UPD-650, UK) with two graphite targets and one chromium target. Briefly, the steel substrates were cleaned with ethanol or petroleum ether. Then, Ar plasma etching was conducted to remove the residual contaminants on the substrate surfaces. A Cr interlayer of ca. 200 nm was deposited on the surface of the steel substrates to enhance the adhesion of the DLC film. The DLC film was deposited using two graphite targets at 3.5 A current. The as-prepared DLC film had a total thickness of approximately 1.8 μm and an intensity ratio of Raman D peak and G peak (I_D/I_G) was 1.34 (Fig. 1(a)). A high I_D/I_G value suggested the presence of a significant quantity of sp^2 cluster structures within the DLC carbon network

2.3 Characterizations

Raman spectra were collected via a confocal Raman spectrometer (InVia™, Renishaw, UK) with an excitation wavelength of 532 nm. An optical microscope (Axio Lab. A1, ZEISS, Germany) and a field emission scanning electron microscope (FE-SEM; Mira 3, Tescan, Czech Republic) were used to observe the worn surfaces of the steel friction pair. An energy-dispersive X-ray spectroscope (EDS; Quantax, Bruker, USA) was used to analyze the compositions of the friction surfaces. The hardness and elastic modulus of the DLC film were measured via a nanoindentation instrument (NHT2, Anton Paar, Austria) at a constant load of 5 mN, with an indentation depth of less than 160 nm, which were 13.6 and 154 GPa, respectively. The optical topography of the worn surfaces of the DLC film was measured via a white light interferometer (ContourGT-K, Bruker, USA). X-ray photoelectron spectroscopy (XPS) was performed on a spectrometer (Escalab 250Xi, Thermo Fisher Scientific, USA) equipped with a monochromatic Al Kα X-ray source. The C–C/C–H component of the C 1s peak at 284.8 eV was used for binding energy calibration of all the elements.

2.4 Tribological evaluation

Friction tests were conducted in an ambient environment on a reciprocating ball-on-disk CSM tribometer equipped with a WPS200-8010 DC power supply. The power supply features an

Table 1 Kinematic viscosity of the four base oils at 100 °C

Type	Viscosity (cSt)
Mineral oil	6.23
PAO6 oil	5.80
Rapeseed oil	8.70
Castor oil	17.20

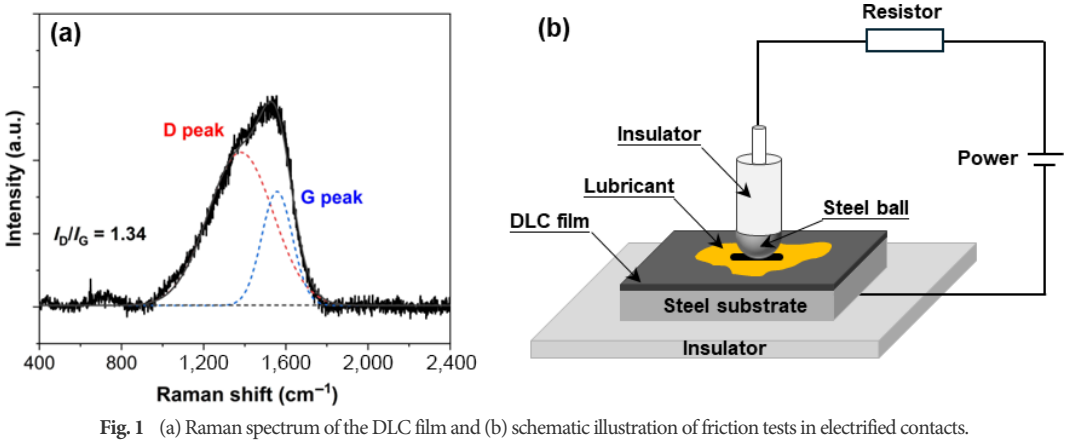

Fig. 1 (a) Raman spectrum of the DLC film and (b) schematic illustration of friction tests in electrified contacts.

output voltage range from 0 to 80 V and an output current range from 0 to 10 A. The positive and negative terminals of the power supply were connected to the steel ball and DLC-coated disk, respectively (Fig. 1(b)). During friction testing, the voltage was monitored in real time via Matrix DC Source software to calculate the contact resistance at the contact point via Ohm's law. The power supply selectively transmitted current only to the contact interface and insulated other components of the tribometer. Bearing steel (GCr15) balls with a diameter of 6 mm and DLC-coated bearing steel disks were used as upper and lower friction pairs, respectively. The normal loads were 5, 10, 15, and 20 N, corresponding to initial maximum Hertz contact stresses between 1.0 and 1.6 GPa. The reciprocating frequency was 5.0 Hz, and the sliding stroke was 5.0 mm. One hundred microliters of mineral, PAO6, rapeseed, or castor oil was introduced into the sliding interface. Currents of 0, 0.5, 1.0, and 1.5 A were applied to the lubricated contact interface. Short-duration (4,000 s) and long-duration (20,000 s) sliding tests were performed to evaluate the electrified friction and wear properties of the DLC film. Friction tests under various conditions were carried out independently at least twice. A stylus-type surface profilometer (KLA-Tencor D-100) was used to determine the wear profiles of the DLC films.

3 Results and discussion

3.1 Electrified friction and wear properties

Figure 2 shows the friction curves of the DLC film against steel balls in four lubricants, both under unelectrified and electrified conditions, in short-duration tests (4,000 s). Under unelectrified conditions, the friction curves of the four lubricants were smooth throughout the test. The electric current led to a minor friction reduction (ca. 5%–20%) for mineral, PAO6, and castor oils but a marginal increase (less than 15%) for rapeseed oil. Notably, the electrified friction was unstable or exhibited sticking characteristics, especially for ester oils at high currents. This result suggested that the electric current changed the interfacial interactions during sliding. In addition, the electrified friction in lubricated contacts is weakly dependent on the lubricant type. Hydrocarbon lubricants possessing varying molecular compositions displayed comparable friction characteristics, whereas ester lubricants formulated with different ingredients presented distinct friction properties. This finding indicates that the molecular structure of lubricants affects the electrified friction behavior of the DLC/steel interface to some extent.

The wear surfaces of the DLC films were observed via white light interference microscopy. Figure 3 shows the optical topography of the wear tracks on the DLC film. Under unelectrified conditions, the DLC film experienced the most severe wear when lubricated with rapeseed oil (Fig. 3(c1)). Wear was undetectable for mineral oil, PAO6, and castor oil, particularly in the case of castor oil. The high degree of wear of the DLC film in rapeseed oil is likely related to its residual organic acid components, which cause chemical or corrosion wear [29, 30]. After the electrified friction tests, protruding tribolayers formed on the DLC surfaces. The ester oils facilitated more pronounced tribo-layer growth. From the cross-sectional profiles of the wear tracks in the insets, these protruding tribolayers have the potential to shield the DLC film from wear in most scenarios. A comparison of the four lubricants revealed that ester oils with highly reactive groups (C=C, C–OH, and O–C=O) were more conducive to the growth of tribolayers on DLC surfaces in the presence of an electric current.

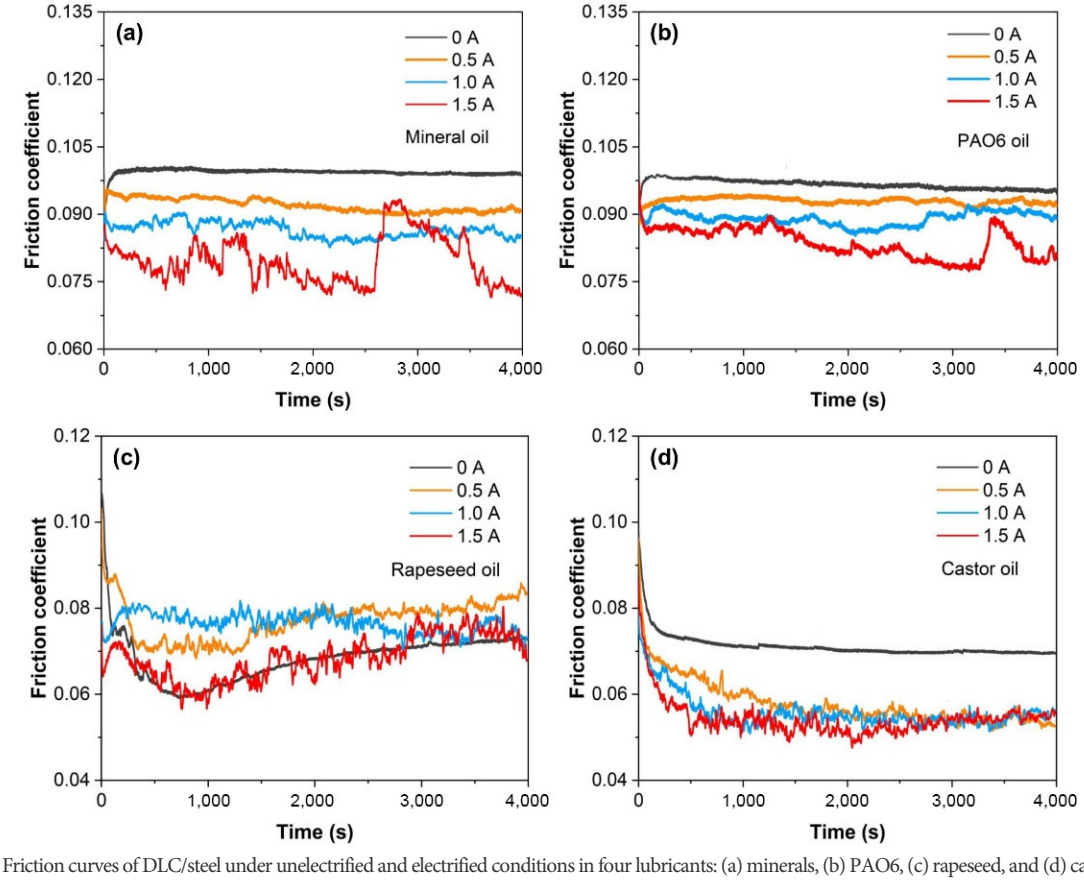

Fig. 2 Friction curves of DLC/steel under unelectrified and electrified conditions in four lubricants: (a) minerals, (b) PAO6, (c) rapeseed, and (d) castor oils.

3.2 Analysis of worn surfaces

After short-duration tests, the worn steel ball surfaces were observed via optical microscopy. Figure 4(a) shows optical photographs of the worn surfaces of the steel balls. A dark tribolayer was formed on the steel ball surfaces for all the lubricants in the electrified contacts. Under unelectrified conditions, hydrocarbon oils, especially mineral oil, form a thin, dark tribolayer on steel surfaces. There was no observable tribo-

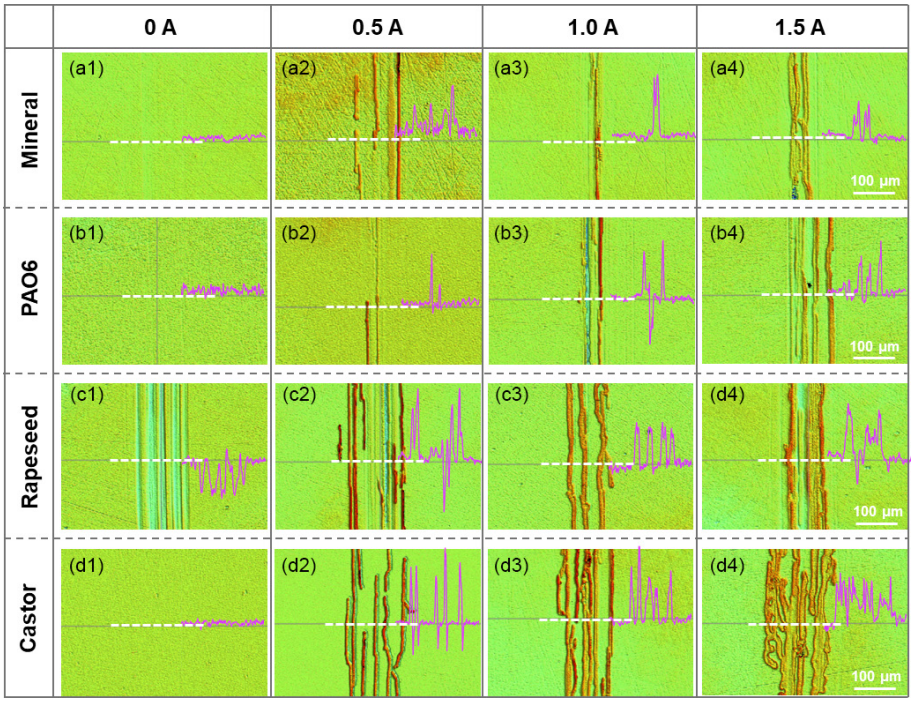

Fig. 3 Optical topography of worn DLC surfaces under varying currents: (a1, d1) 0 A, (a2, d2) 0.5 A, (a3, d3), 1.0 A, and (a4, d4), 1.5 A lubricated with four lubricants: (a) mineral, (b) PAO6, (c) rapeseed, and (d) castor oils. The insets are the cross-sectional profile of the worn DLC surface extracted from the white dashed lines.

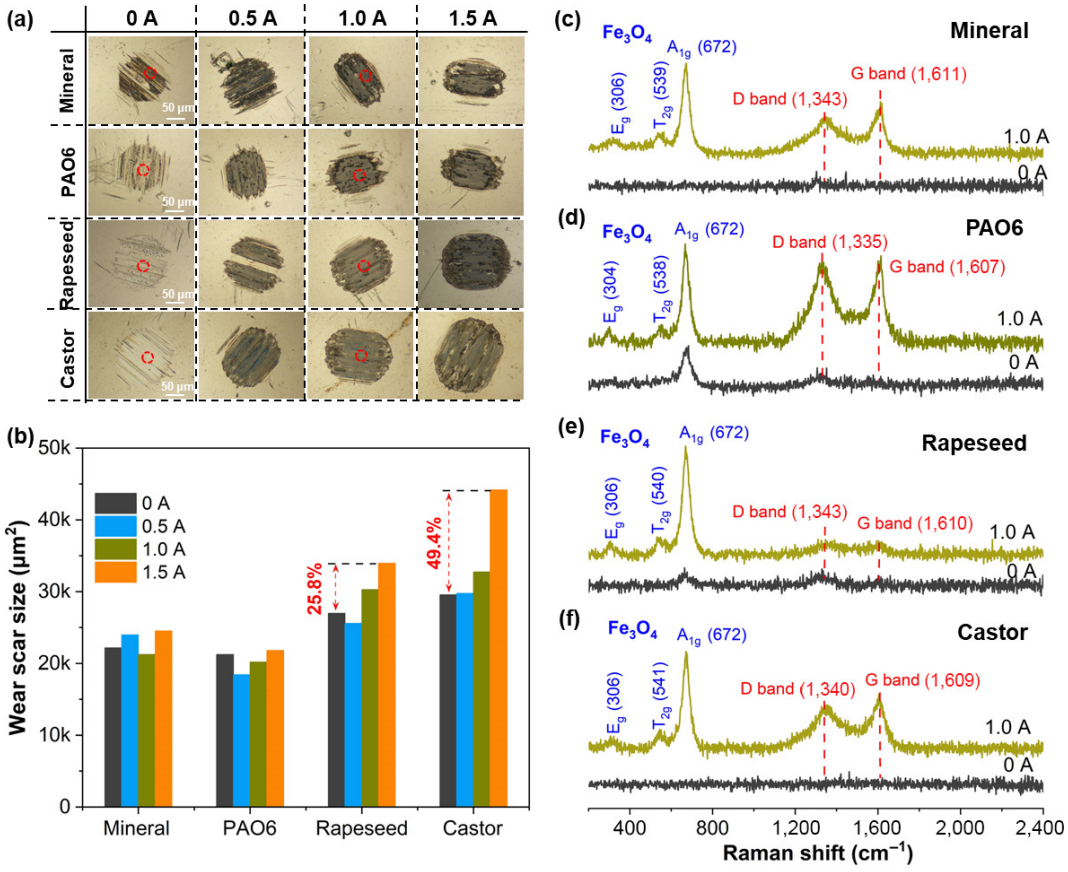

Fig. 4 (a) Optical photographs and (b) size of wear scars on steel balls under varying currents in four lubricants. (c–f) Raman spectra obtained from wear scars on steel balls following sliding for 4,000 s at 0 and 1.0 A currents. The spectral measurement area is marked with red dashed circles.

layer for the two ester lubricants because of their strong adsorption capacity, good dispersion ability to wear products, or acid-promoted tribo-chemical reactions. Given that lubricants can hinder the creation of a carbon transfer layer on the steel surface in lubricated DLC/steel contact [31, 32], the tribo-layer in electrified contacts may be attributed to the oxidation of the steel pair and/or the degradation of lubricants. Figure 4(b) shows the size of the wear scars on the steel balls. The scars for the ester oils tended to increase in size as the electric current increased. Specifically, at 1.5 A, the wear scar sizes increased by approximately 25% and 49% for rapeseed and castor oils, respectively. These findings suggested that the ester oils exacerbated the wear of the steel pair in the electrified DLC/steel contact, particularly under high current conditions. Given the fatty acids in ester lubricants, the electrically promoted galvanic corrosion may explain the observed wear behavior of the steel balls [33, 34].

Raman spectra were acquired to understand the electrified friction behavior. Figures 4(c)–4(f) show the Raman spectra of the wear scars at 0 and 1.0 A. Under no current conditions, weak Raman signals were detected at approximately 670, 1,340, and 1,610 cm^{-1} for PAO6 and rapeseed oils, which can be assigned to the A_{1g} mode of magnetite (Fe_3O_4) and the D band and G band of graphite-like carbon, respectively [35–38]. At 1.0 A, Raman peaks at approximately 305, 540, and 670 cm^{-1} corresponded to the E_g, T_{2g}, and A_{1g} modes of Fe_3O_4, respectively, which was observed for all lubricants [35, 36]. The D and G bands of graphite-like carbon were evident for different oils, with the exception of rapeseed oil. This meant that the electric current promoted the tribo-oxidation of steel pairs and the formation of graphite-like carbon, forming tribolayers containing iron oxides and graphitized carbon. Owing to their molecular structures, the four lubricants had somewhat distinct compositions of tribolayers. For example, the tribolayer from rapeseed oil mainly consists of iron oxides, resulting in a weak graphitized carbon signal.

Figure 5 shows optical photographs of the wear tracks formed on the DLC surface at 0 and 1.0 A currents after sliding for 4,000 s. Under unelectrified conditions, wear surfaces with grooves were observed for all lubricants. The most severe DLC wear occurred for rapeseed oil, which was related to chemical or corrosion wear caused by its organic acid components [33, 39]. Under electrified conditions, the DLC surfaces presented striated tribolayers in tracks, which became especially prominent in the cases of ester oils and high currents (corresponding to surface-protruding growth in Fig. 3). Localized DLC peeling was another notable feature under electrified conditions, particularly at higher currents (Figs. 5(a3)–5(d3)). This meant that the electric current induced peeling damage to the DLC film. This observation was in accordance with the previously reported failure of an H-free tetrahedral carbon film in lubricated electrified contacts [26]. Given the protruding features of the tribolayers, electrically induced lubricant degradation may generate such tribolayers.

Figures 5(a4)–5(d4) show the Raman spectra of worn DLC surfaces obtained from areas numerically labeled on the surfaces of the wear tracks. Without current, the worn DLC surfaces (circled 1) displayed an asymmetric Raman peak regardless of lubricant type, indicative of the amorphous characteristic of the original DLC carbon network (Fig. 1(a)). Under electrified conditions, the scratched DLC surfaces (circled 2) in the four oils presented asymmetric Raman peaks analogous to those of the original DLC film. However, those protruding tribolayers (circled 3) featured two separate Raman peaks at approximately 1,350 and 1,600 cm^{-1}, indicating the formation of graphite-like carbon on the DLC surfaces [37]. Since no notable DLC wear was detected in the

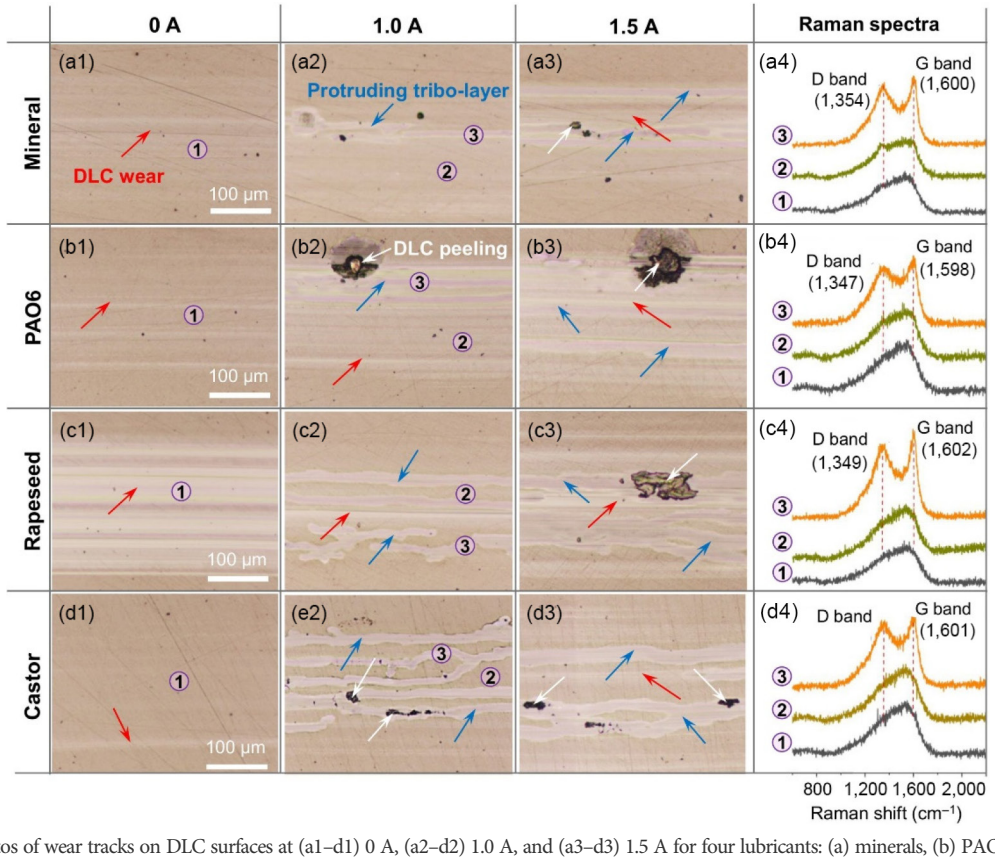

Fig. 5 Optical photos of wear tracks on DLC surfaces at (a1–d1) 0 A, (a2–d2) 1.0 A, and (a3–d3) 1.5 A for four lubricants: (a) minerals, (b) PAO6, (c) rapeseed, and (d) castor oils. (a4–d4) Raman spectra of numerically marked areas on worn DLC surfaces.

electrified contacts, these protruding graphite-like tribolayers were attributed to lubricant degradation rather than electrically induced graphitization of the DLC network. This suggested that at a lubricated DLC/steel interface, the current-induced resistance heat and arc effect may facilitate the degradation of lubricants, thereby forming a graphitized carbon layer on the surface of the DLC.

Additional Raman analysis was conducted on the peeled areas on the DLC surfaces to gain insights into the DLC damage behavior. As depicted in Figs. 6(a)–6(d), Raman spectra were acquired from the central and edge zones of the worn DLC surface within the peeling region. Compared with the central zones, the edge zones presented more pronounced graphitization characteristics. Furthermore, a strong fluorescent background was observed in the Raman spectra, particularly for the edge zones. Consequently, arc ablation may have induced peeling of the DLC film, which was accompanied by intense chemical interactions between the DLC and the lubricant.

The Raman spectra in Fig. 4 confirmed the analogous tribolayers containing iron oxides and graphite-like carbon on the steel ball surfaces under electrified conditions. Figure 7 further shows the SEM images and elemental compositions of the worn steel ball surfaces at 0 and 1.0 A currents when lubricated with the four lubricants. From the SEM images (Figs. 7(a1)–7(d1)), the plowing effect was evident for all lubricants in the absence of current. At a current of 1.0 A, the plowing action was inhibited, and the adhesive formed a tribo-layer (Figs. 7(a2)–7(d2)). This result indicated that the electric current induced a transition in the friction mechanism from abrasion to adhesion. Figure 7(e) shows the chemical compositions of the wear scars in Figs. 7(a)–7(d), which were obtained via EDS. The friction surfaces mainly contained Fe, C, and O. Compared with those of the unelectrified samples, the electrified friction surfaces (1.0 A) had a lower Fe content and higher C and O concentrations. The increase in O content was the most significant change in composition, which demonstrated the tribo-oxidation of the steel friction pairs (Figs. 4(c)–4(f)). Despite the increased tribo-oxidation, the oxidative wear of the steel pair seemed to be insignificant in the short-term test, especially at low currents (Fig. 4(b)).

Figure 8 presents the XPS spectra of the wear scars formed on the steel surfaces at currents of 0 and 1.0 A when lubricated with PAO6 and rapeseed oil. The C 1s spectrum exhibited four distinct peaks at approximately 283.2, 284.8, 286.2, and 288.1 eV, which were assigned to C–Fe, C–C/C–H, C–O, and C=O bonds, respectively [40]. The electric current did not affect the proportions of C–O and C=O in the rapeseed oil, with a slight increase in PAO6 lubrication. Analysis of the O 1s spectra revealed an elevated O–Fe peak (529.8 eV) ratio for PAO6 at 1.0 A, suggesting tribo-oxidation of the steel surfaces. Conversely, for rapeseed oil, the enhanced O–C peak was noted, which might be related to the chemical adsorption of ester molecules onto the tribo-layer. The Fe 2p spectra provided evidence for the existence of Fe(III) and Fe(0), with Fe(0) being relevant to the area outside the wear scar. Notably, the attenuated satellite peak at ~719.7 eV in the Fe 2p spectra signified the formation of Fe_3O_4 under electrified conditions [41], which was consistent with the Raman data presented in Fig. 4.

3.3 Influence of loads

To further probe the electrified friction of the DLC/steel contact, sliding tests were conducted at 0 and 1.0 A currents under varying loads. Figures 9(a)–9(d) depict the friction curves obtained for the four lubricants. Under electrified and unelectrified conditions, the friction coefficient of the mineral, PAO6, and castor oils tended to increase with increasing load. For rapeseed oil, the friction had a weak dependence on load and even tended to decrease as the load increased under electrified conditions. The increase in solid-solid contact generally accounts for the elevated friction as the load increases [42]. The strong adsorption of polar fatty acids could explain the observed friction behavior of rapeseed oil [43]. The electrification gave rise to friction and caused friction instability. Figures 9(e)–9(h) present optical photos of worn DLC surfaces at various loads at 1.0 A. The electrically induced tribo-layer prevented the wear of the DLC film at low loads. At high loads, despite the existence of the tribo-layer, the DLC film exhibited observable wear, particularly when ester oils were used. Furthermore, a high load promoted peeling wear in the DLC film (Figs. 9(d) and 9(f)).

3.4 Long-duration tests

Given the unstable electrified friction characteristics and observed

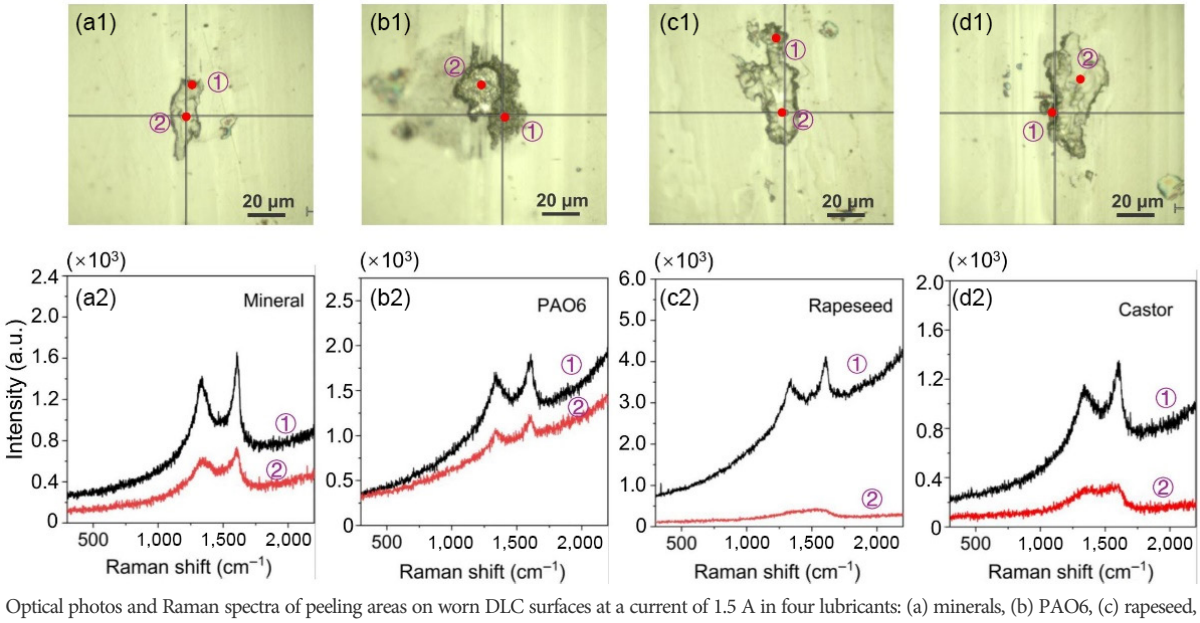

Fig. 6 Optical photos and Raman spectra of peeling areas on worn DLC surfaces at a current of 1.5 A in four lubricants: (a) minerals, (b) PAO6, (c) rapeseed, and (d) castor oils.

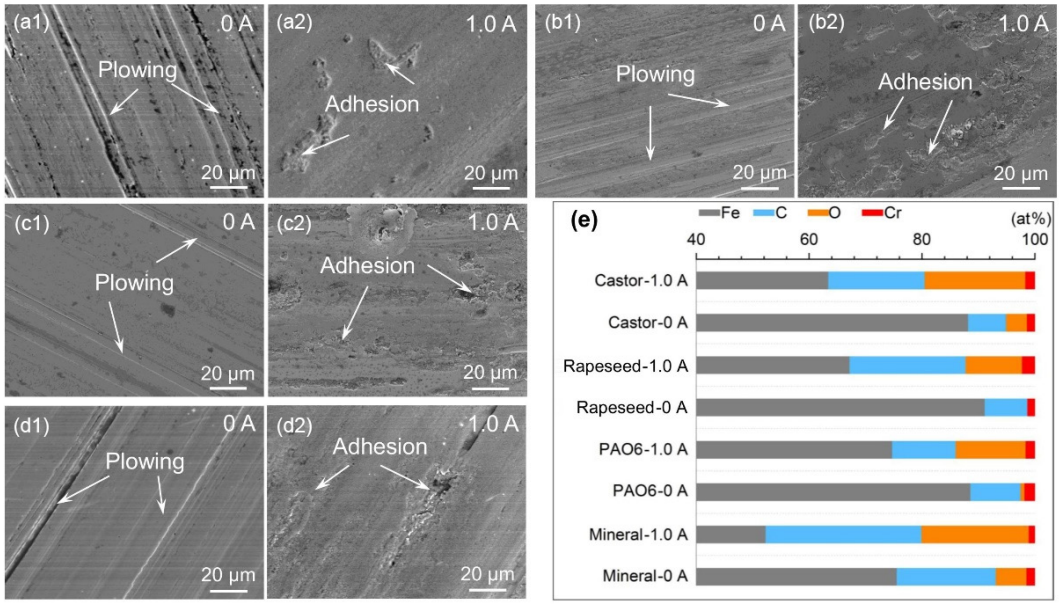

Fig. 7 SEM images of wear scars on steel balls formed at 0 and 1.0 A current for four lubricants: (a) minerals, (b) PAO6, (c) rapeseed, and (d) castor oils. (e) EDS composition of the wear scars in (a–d).

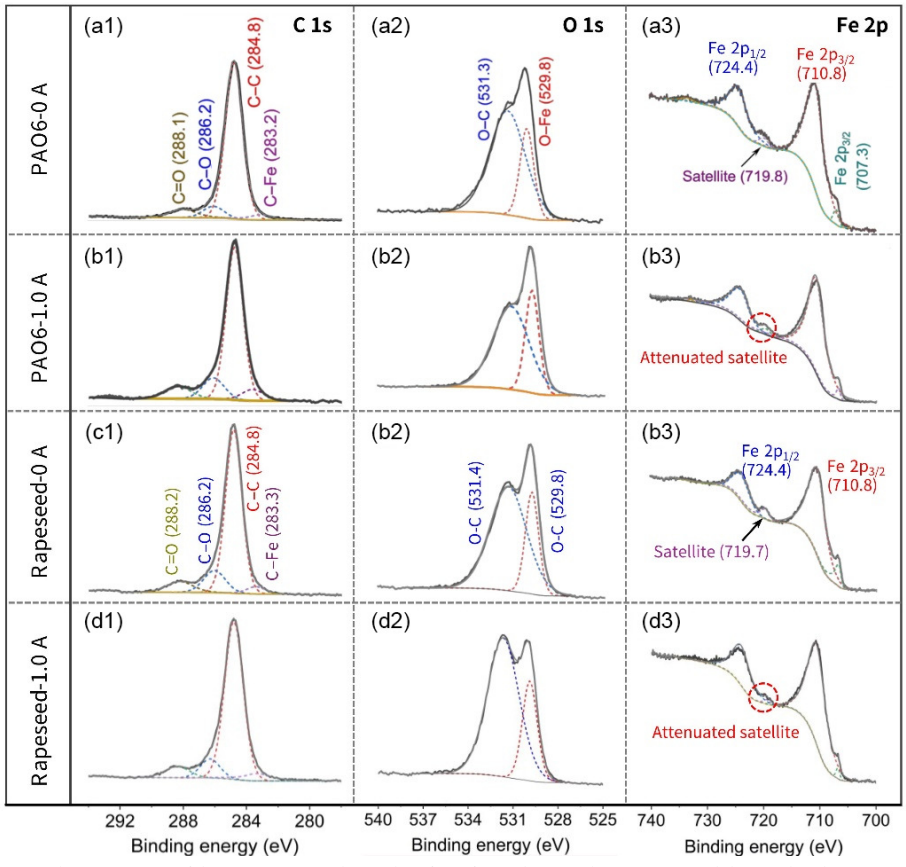

Fig. 8 Fitted XPS C 1s, O 1s, and Fe 2p spectra of the wear scars on the steel surfaces formed at 0 and 1.0 A currents lubricated with PAO6 and rapeseed oil: (a) PAO6-0A, (b) PAO6-1.0A, (c) rapeseed-0A, and (d) rapeseed-1.0A.

peeling damage, long-duration friction tests (20,000 s) were conducted with different lubricants at currents of 0 and 1.0 A. Figures 10(a) and 10(b) display the friction curves. Friction remained the primary characteristic under electrified conditions. At the beginning stage of sliding, the friction values for the mineral, PAO6, and castor oils at 1.0 A were lower than those of the unelectrified samples, which aligns with the short-duration tests depicted in Fig. 2. However, as sliding continued, the electrified friction level in PAO6 exceeded that in the unelectrified scenario. Moreover, the electrification friction in rapeseed oil was slightly greater than that in the unelectrified state. These findings indicate that PAO6 and rapeseed oils exhibited slightly degraded lubricating performance under electrified conditions.

Figure 10(c) shows optical photographs of the scars on steel

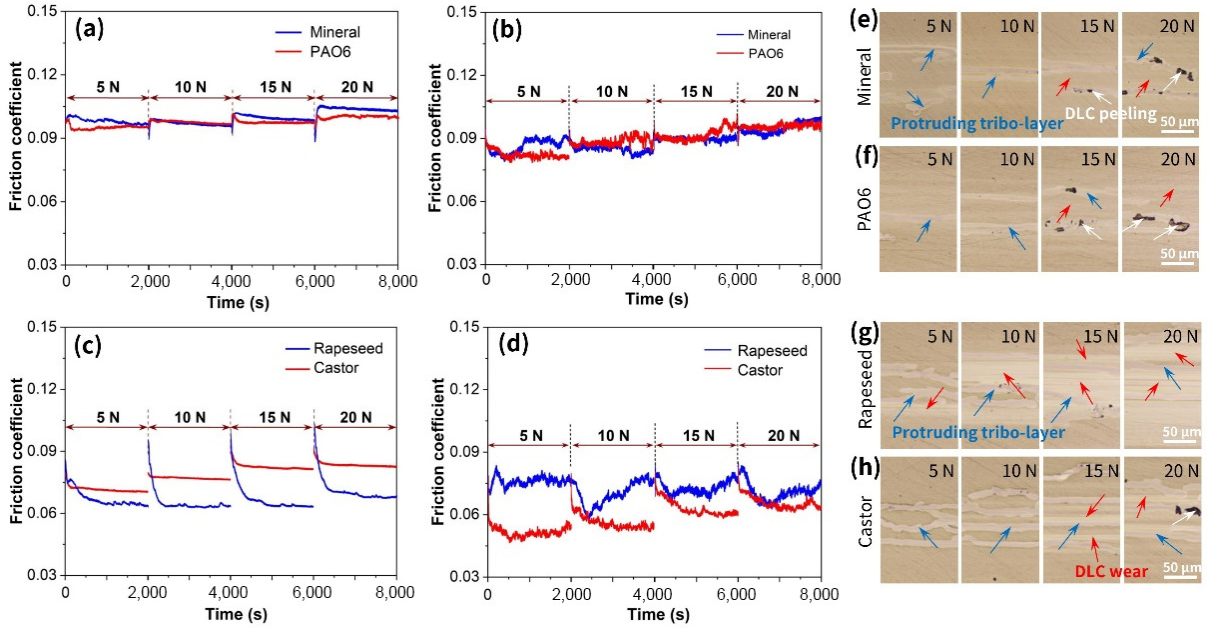

Fig. 9 Friction curves of DLC/steel contact at 0 and 1.0 A currents under varying loads in four lubricants: (a) mineral and PAO6 oils-0 A, (b) mineral and PAO6 oils-1.0 A, (c) rapeseed and castor oils-0 A, and (d) rapeseed and castor oils-1.0 A. (e)–(h) Optical photos of wear tracks on the DLC surface formed at 1.0 A under different loads.

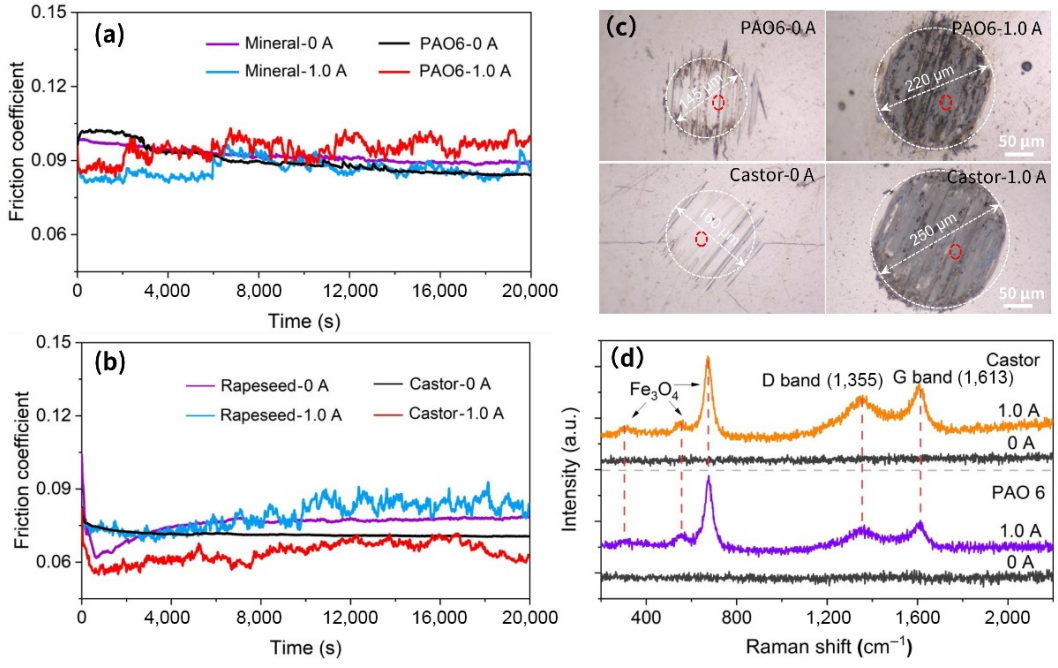

Fig. 10 Friction curves of DLC/steel in long-duration tests at 0 and 1.0 A currents in different lubricants: (a) minerals and PAO6 and (b) rapeseed and castor oils. (c) Optical photos and (d) Raman spectra of scars on steel balls lubricated with PAO6 and castor oils after long-term tests.

balls lubricated with PAO6 and castor oils after sliding for 20,000 s at 0 and 1.0 A currents. No discernible tribo-layer was observed on the steel ball surfaces under unelectrified conditions. At 1.0 A, a dark tribolayer was evident on the worn steel ball surfaces, tallying with the observation in Fig. 4(a). Notably, the scars formed under electrified conditions significantly increased in size, with a 130% increase for PAO6 and a 144% increase for castor oil. Figure 10(d) shows the Raman spectra collected from the wear scars shown in Fig. 10(c). In the absence of current, the Raman spectra lacked identifiable features. At 1.0 A, the Raman spectra exhibited similar characteristics to those in Figs. 4(c)–4(f), suggesting the same material evolution. The long-duration sliding did not introduce novel structural changes on the steel surface.

After the long-duration tests, the tracks on the DLC surface were examined via optical microscopy. Well-defined wear marks were visible on the DLC surface under unelectrified conditions (Figs. 11(a1)–11(d1)), with no signs of DLC peeling failure. At 1.0 A, significant peeling failure occurred on the worn DLC surfaces (Figs. 11(a2)–11(d2)). Compared with the tracks in short-duration tests, long-duration sliding resulted in more obvious DLC peeling. When lubricated with hydrocarbon oils, the steel substrate was especially clear in the peeling zones. This could be related to the fewer protruding tribolayers on the DLC surface in hydrocarbon oils, which increased the local contact stress and reduced the number of channels for current transmission across the contact interface. In addition to their low electrical conductivity, this

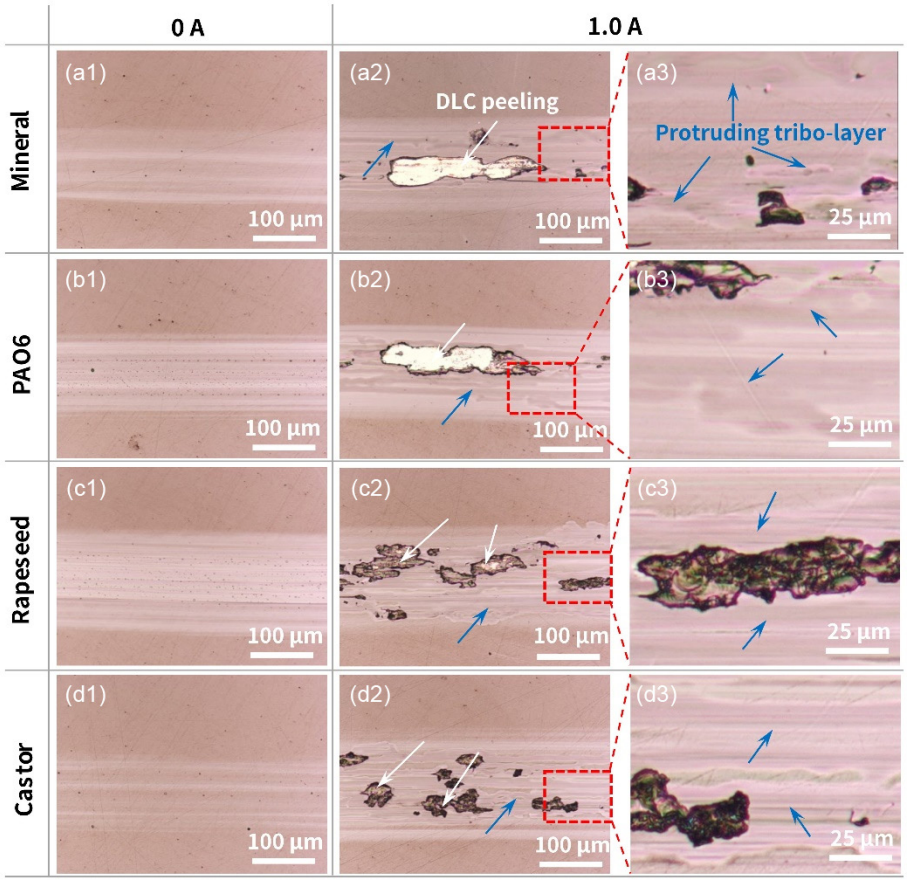

Fig. 11 Optical photos of wear tracks formed on the DLC surface after 100,000 laps of sliding at 0 and 1.0 A current in four lubricants: (a) mineral oil, (b) PAO6, (c) rapeseed oil, and (d) castor oil. (a_3–d_3) Enlarged photos of the selected area in (a_2–d_2).

resulted in increased arc ablation, resulting in peeling of the DLC. Additionally, from the enlarged photos in Figs. 9(a3)–9(d3), the growth of the tribo-layer on the DLC surface became particularly significant under electrified conditions, especially in the case of ester oils. Notably, as shown in Figs. 5, 7, and 11, the electric current-induced DLC peeling occurred primarily in the areas where the tribo-layer developed. These protruding tribolayers served as the primary contact points and main channels for current transmission, which were susceptible to locally generating more concentrated Joule heat and were prone to induce arc ablation, thereby causing peeling damage to the DLC film.

3.5 Possible mechanisms for electrified friction and wear

To understand the electrified tribological behavior, friction tests were carried out by intermittently applying current. Figures 12(a) and 12(b) illustrate the friction variation in the four lubricants. The sliding experiments started with a current of either 0 or 1.0 A for 5,000 laps, subsequently switching to 1.0 or 0 A, respectively, for another 5,000 laps, with this sequence repeated. Intriguingly, when no electric current was applied, the friction curves exhibited smooth profiles and yielded elevated friction values. This indicated that the electric current altered the interfacial interactions, as evidenced by the friction reduction. The abrupt change in friction upon the application of current suggested that the electric field across the contact zone might modify the nature of the interfacial interactions [44]. This finding also confirmed that the sticking friction in electrified contacts was not due to the uneven growth of tribolayers on the DLC surfaces (Fig. 3), which may cause friction instability. The contact resistance of the sliding interfaces was measured by monitoring the contact voltage (the resistor in Fig. 1(b) was zero ohms), utilizing Ohm's law. Figures 12(c) and 12(d) depict the variations in contact resistance during sliding when lubricated with the four lubricants. The interfaces under different lubrication conditions had comparable contact resistance values ranging from 1.1 to 2.2 Ω, corresponding to a contact voltage range of 1.1 to 1.7 V. The contacts at high currents exhibited lower contact resistance due to the enhanced interface contact facilitated by the increased Joule heat and other factors.

On the basis of the previous results, an electrified friction and wear mechanism can be proposed for lubricated DLC/steel contact (Fig. 13). During friction, real contact occurs among the microasperities. This can lead to significantly increased contact resistance at the sliding interface. Thus, the main voltage drops in the electrified contacts will occur at the sliding interface [44]. An electric field can be produced between friction surfaces, which not only causes electron redistribution on the sliding surfaces but also adjusts the configuration of lubricant molecules at the contact interface [45, 46]. This changes the adsorption and induces the polarization of surface charges and lubricant molecules. The liquid molecules could even be arranged in an ordered structure on friction surfaces [47]. Jiang et al. [48] noted that the voltage-induced polarization of charges could cause intensive electrostatic interactions between a Pt-coated Si tip and graphene oxide films, leading to a corresponding rise in adhesive and frictional forces. Therefore, in electrified DLC/steel contact, the sliding interface transformed from DLC/steel to oxidized tribo-layer/carbon as the sliding progressed (Figs. 4 and 5). For the oxidized tribo-layer, the electric field across the contact could polarize surface C–O and Fe–O bonds (Fig. 8). The polarized surface facilitated the adsorption of the polarized lubricant molecules and thereby

helped form a lubricant film at the sliding interface. However, for the DLC surface, the electric field did not induce a significant dipole change in the nonpolar or weakly polar C–C/C=C bonds, which had a small effect on the adsorption behavior of the lubricant on the DLC surface. This may explain the lower friction level under electrified conditions (Figs. 12(a) and 12(b)). On the other hand, the dynamic electric field across the contact caused electrostatic interactions due to the polarization of charges, thereby sticking friction on account of adhesive forces and other physical interactions, such as molecular chain entanglement. In terms of peeling damage to the DLC film, the protruding tribo-layer on the DLC surface dominates the contact and contracts the current channel, which generates more concentrated Joule heat and arc effects, thereby leading to peeling failure due to thermal stress at the DLC film/substrate interface.

4 Conclusions

This study investigated the electrified tribological behavior of a highly sp^2 hybridized H-free DLC film with a Cr interlayer under

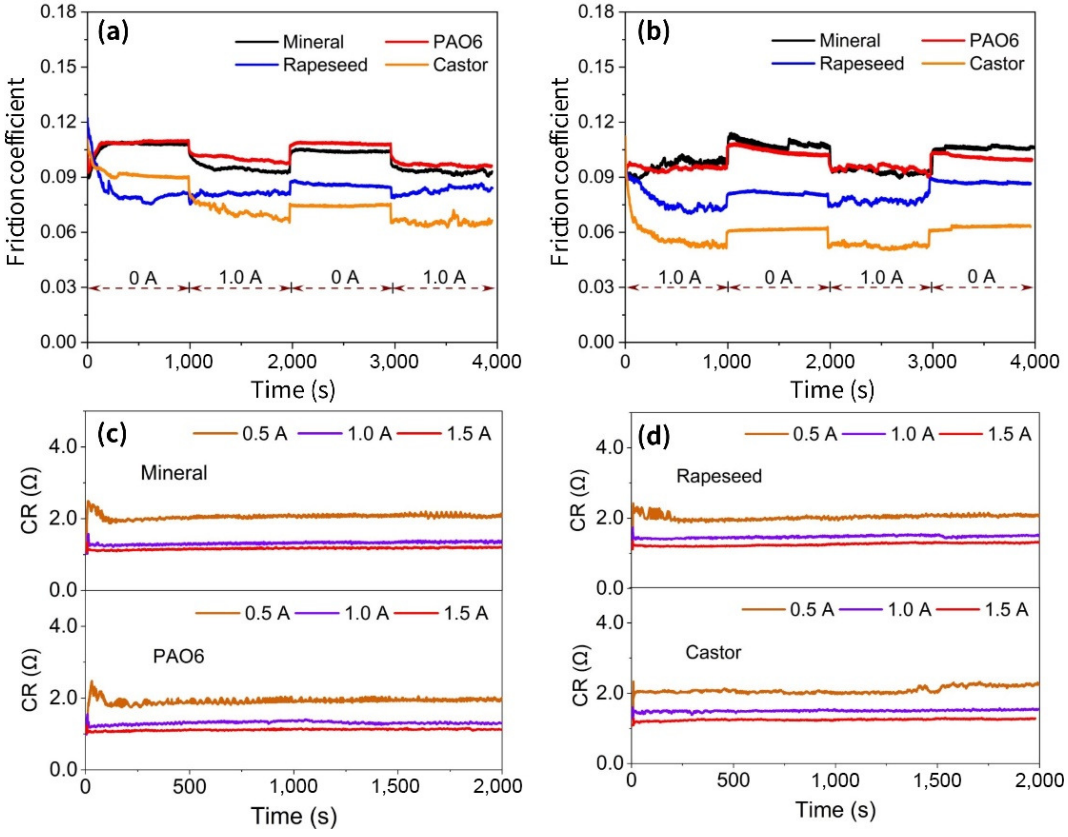

Fig. 12 (a, b) Friction curves of DLC/steel in four lubricants with intermittent current supply. (c, d) Contact resistance (CR) at the electrified DLC/steel interface during sliding.

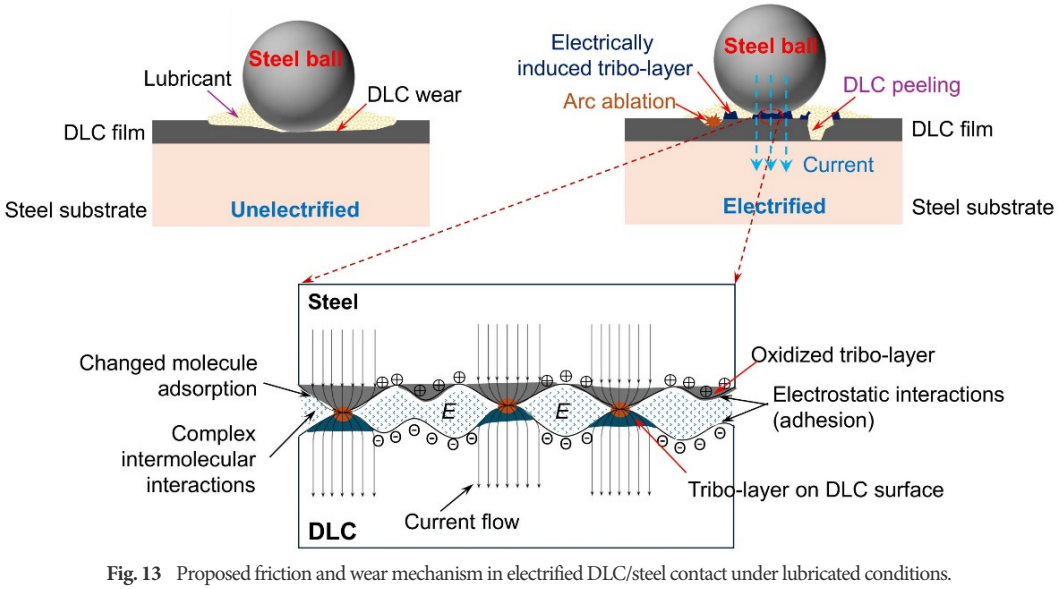

Fig. 13 Proposed friction and wear mechanism in electrified DLC/steel contact under lubricated conditions.

lubricated conditions. The friction surfaces were characterized to scrutinize the electrically promoted tribological changes at the lubricated DLC/steel interface. The main conclusions are as follows:

(1) The electric current caused sticking and unstable friction in the lubricated DLC/steel contact, regardless of the lubricant type used. This could be attributed to the adhesion and intermolecular interactions induced by the electric field across the contact. Depending on the specific lubricant and test duration, minor friction variations, increasing or decreasing, were noted upon the application of an electric current.

(2) The electric current triggered graphite-like tribolayer growth on the DLC surface as a result of lubricant degradation, particularly in ester oils with reactive groups (e.g., C=C, C–OH, O–C=O), which mitigated DLC wear to some extent. However, the electric current also caused the DLC peeling due to arc ablation and resistive heating, suggesting the deteriorated availability of the DLC film in electrified sliding components. This underscores the necessity for further research to investigate the influence of DLC film variables (e.g., the type of metal interlayer) on electrified tribological behavior.

(3) The tribo-oxidation of the steel pair and the degradation of lubricants constitute the primary material evolution in the electrified DLC/steel contacts. Tribo-oxidation expedited the wearing process of the steel pair, whereas the degradation of the lubricant had no significant detrimental influence on the friction surfaces.

Acknowledgements

This work was supported by the Strategic Priority Research Program of the Chinese Academy of Sciences (No. XDB0470202) and the Major Science and Technology Project of Gansu Province (No. 23ZDGA011).

Declaration of competing interest

The authors have no competing interests to declare that are relevant to the content of this article.

References

[1] Li S B, Yang X Z, Kang Y Q, Li Z Y, Li H W. Progress on current-carry friction and wear: An overview from measurements to mechanism. *Coatings* **12**(9): 1345 (2022)

[2] Fu Y, Qin H L, Xu X, Zhang X L, Guo Z G. What are the progresses and challenges, from the electrical properties of current-carrying friction system to tribological performance, for a stable current-carrying interface. *J Bio Tribo Corros* **8**(1): 4 (2021)

[3] Sun K, Diao D F. Current density effect on current-carrying friction of amorphous carbon film. *Carbon* **157**: 113–119 (2020)

[4] Yang Z H, Song Y J, Jiao J L, Li W B, Shangguan B, Zhang Y Z. Optimization of current-carrying friction and wear properties of copper-carbon composite materials based on damage. *Tribol Int* **191**: 109074 (2024)

[5] Zhou Y K, Du M D, Zuo X. Influence of electric current on the temperature rise and wear mechanism of copper–graphite current-carrying friction pair. *J Tribol* **144**(10): 101701 (2022)

[6] Wu R X, Song C F, Wu H H, Lv B, Zhang Y Y, Zhang Y Z. Effect of relative humidity on the current-carrying tribological properties of Cu–C sliding contact pairs. *Wear* **492–493**: 204219 (2022)

[7] Du J B, Lu M C, Fang J M, Li W, Chen D X. Current-carrying friction behavior and wear mechanism of Ag coatings by rotary spray deposition. *Wear* **546–547**: 205367 (2024)

[8] Huang Q R, Song C F, Liu Z L, Hou X B, Pang X J, Sun C, Lu H H, Wang S, Zhang Y Z. Research progress on the characteristics of current-carrying tribology in electrical transmission. *Space Sol Power Wirel Transm* **1**(1): 37–47 (2024)

[9] Kolawole F O, Kolade O S, Bello S A, Kolawole S K, Ayeni A T, Elijah T F, Borisade S G, Tschiptschin A P. The improvement of diamond-like carbon coatings for tribological and tribo-corrosion applications in automobile engines: An updated review study. *Int J Adv Manuf Technol* **126**(5): 2295–2322 (2023)

[10] Rajak D K, Kumar A, Behera A, Menezes P L. Diamond-like carbon (DLC) coatings: Classification, properties, and applications. *Appl Sci* **11**(10): 4445 (2021)

[11] Humphrey E, Elisaus V, Rahmani R, Mohammadpour M, Theodossiades S, Morris N. Diamond like-carbon coatings for electric vehicle transmission efficiency. *Tribol Int* **189**: 108916 (2023)

[12] Erdemir A, Donnet C. Tribology of diamond-like carbon films: Recent progress and future prospects. *J Phys D: Appl Phys* **39**(18): R311–R327 (2006)

[13] Al Mahmud K A H, Kalam M A, Masjuki H H, Mobarak H M, Zulkifli N W M. An updated overview of diamond-like carbon coating in tribology. *Crit Rev Solid State* **40**(2): 90–118 (2015)

[14] Evaristo M, Fernandes F, Cavaleiro A. Influence of the alloying elements on the tribological performance of DLC coatings in different sliding conditions. *Wear* **526–527**: 204880 (2023)

[15] Yu Q Y, Chen X C, Zhang C H, Luo J B. Influence factors on mechanisms of superlubricity in DLC films: A review. *Front Mech Eng* **6**: 65 (2020)

[16] Liang H T, Yang X, Yue C T, Zhao G Z, Zhang J Y, Wang Y F. A comparative friction and wear study of diamond and diamond-like carbon films against Cu. *Tribol Int* **193**: 109344 (2024)

[17] Wang W, Huang X, Huang Y Q, Wang Y. Nanoscale friction of tetrahedral amorphous diamond-like carbon film after thermal annealing. *Tribol Int* **190**: 109064 (2023)

[18] Lawes S A, Fitzpatrick M E, Hainsworth S V. Evaluation of the tribological properties of DLC for engine applications. *J Phys D Appl Phys* **40**(18): 5427–5437 (2007)

[19] Hofmann D, Kunkel S, Bewilogua K, Wittorf R. From DLC to Si-DLC based layer systems with optimized properties for tribological applications. *Surf Coat Tech* **215**: 357–363 (2013)

[20] Zeng Q F, Ning Z K. High-temperature tribological properties of diamond-like carbon films: A review. *Rev Adv Mater Sci* **60**(1): 276–292 (2021)

[21] Wang F, Shang L L, Zhang G G, Wang Z F. Polyethylene glycol derived carbon quantum dots nanofluids: An excellent lubricant for diamond-like carbon film/bearing steel contact. *Friction* **10**(9): 1393–1404 (2022)

[22] Chen S S, Song N N, Zhang S M, Zhang Y J, Yu L G, Zhang P Y. Synergistic tribological effect between polyisobutylene succinimide-modified molybdenum oxide nanoparticle and zinc dialkyldithiophosphate for reducing friction and wear of diamond-like carbon coating under boundary lubrication. *Friction* **11**(11): 2021–2035 (2023)

[23] Wang Y F, Wang Y, Li X, Li A, Lu Z B, Zhang G G, Wu Z G. The friction and wear properties of metal-doped DLC films under current-carrying condition. *Tribol T* **62**(6): 1119–1128 (2019)

[24] Xue P D, Chen C, Fan X, Diao D F. Current-carrying friction in carbon coated ball bearing. *Friction* **11**(11): 2008–2020 (2023)

[25] Wang Y F, Luo X B, Wang F, Zhang G G. Interface analysis for diamond-like carbon film sliding against 9Cr18 steel under current-carrying conditions. *Diam Relat Mater* **144**: 111006 (2024)

[26] Farfan-Cabrera L I, Cao-Romero-Gallegos J A, Lee S, Komurlu M U, Erdemir A. Tribological behavior of H-DLC and H-free DLC coatings on bearing materials under the influence of DC electric current discharges. *Wear* **522**: 204709 (2023)

[27] Ding Q, Tang J, Zhang S, Li H, Hu L. The tribological behavior of PAO lubricated DLC contacts under DC electric field. *Tribology* **37**: 707–716 (2017) (in Chinese)

[28] Braceras I, Ibáñez I, Dominguez-Meister S, Velasco X, Brizuela M, Garmendia I. Electro-tribological properties of diamond like carbon coatings. *Friction* **8**(2): 451–461 (2020)

[29] Kalin M, Vižintin J. A comparison of the tribological behaviour of steel/steel, steel/DLC and DLC/DLC contacts when lubricated with mineral and biodegradable oils. *Wear* **261**(1): 22–31 (2006)
[30] Zhang J Y, Liu W M, Xue Q J. The friction and wear behaviors of some O-containing organic compounds as additives in liquid paraffin. *Wear* **219**(1): 124–127 (1998)
[31] Kim D W, Kim K W. Effects of sliding velocity and ambient temperature on the friction and wear of a boundary-lubricated, multi-layered DLC coating. *Wear* **315**(1–2): 95–102 (2014)
[32] Tamura Y, Zhao H, Wang C, Morina A, Neville A. Interaction of DLC and B_4C coatings with fully formulated oils in boundary lubrication conditions. *Tribol Int* **93**: 666–680 (2016)
[33] Hibi Y, Mano H. Tribological behavior of cast iron in ethanol with and without oleic acid. *Tribol Online* **11**(6): 675–680 (2016)
[34] Hibi Y, Mano H. Effect of acetic acid on wear properties of ferrous and titanium-based materials under ethanol lubrication. *Mater Trans* **61**(12): 2419–2427 (2020)
[35] de Faria D L A, Venâncio Silva S, de Oliveira M T. Raman microspectroscopy of some iron oxides and oxyhydroxides. *J Raman Spectrosc* **28**(11): 873–878 (1997)
[36] Wu X, Tang J Y, Zhang Y C, Wang H. Low temperature synthesis of Fe_3O_4 nanocrystals by hydrothermal decomposition of a metallorganic molecular precursor. *Mater Sci Eng B* **157**(1–3): 81–86 (2009)
[37] Liu Y, Erdemir A, Meletis E I. An investigation of the relationship between graphitization and frictional behavior of DLC coatings. *Surf Coat Tech* **86–87**: 564–568 (1996)
[38] Okubo H, Tadokoro C, Hirata Y, Sasaki S. *In situ* Raman observation of the graphitization process of tetrahedral amorphous carbon diamond-like carbon under boundary lubrication in poly-alpha-olefin with an organic friction modifier. *Tribol Online* **12**(5): 229–237 (2017)
[39] Tang J Z, Ding Q, Zhang G G, Hu L T. The influence of total acid number of ester oil in tribological behavior of DLC contacts. *Tribol T* **58**(5): 849–858 (2015)
[40] Chen X N, Wang X H, Fang D. A review on C 1s XPS-spectra for some kinds of carbon materials. *Fuller Nanotub Carbon Nanostruct* **28**(12): 1048–1058 (2020)
[41] Yamashita T, Hayes P. Analysis of XPS spectra of Fe^{2+} and Fe^{3+} ions in oxide materials. *Appl Surf Sci* **254**(8): 2441–2449 (2008)
[42] Cao-Romero-Gallegos J A, Taghizadeh S, Aguilar-Rosas O A, Dwyer-Joyce R S, Farfan-Cabrera L I. The effect of electrical current on lubricant film thickness in boundary and mixed lubrication contacts measured with ultrasound. *Friction* **12**(8): 1882–1896 (2024)
[43] Arnšek A, Vižintin J. Lubricating properties of rapeseed-based oils. *J Synth Lubr* **16**(4): 281–296 (2000)
[44] Timsit R S. Electrical contacts: Scientific fundamentals. In: *Encyclopedia of Tribology*. Wang Q J, Chung Y W. Eds. Boston: Springer, 2013: 903–905.
[45] Song A S, Shi R Y, Lu H L, Wang X Y, Hu Y Z, Gao H J, Luo J B, Ma T B. Fluctuation of interfacial electronic properties induces friction tuning under an electric field. *Nano Lett* **22**(5): 1889–1896 (2022)
[46] Drummond C. Electric-field-induced friction reduction and control. *Phys Rev Lett* **109**(15): 154302 (2012)
[47] Wang Y, Wang J, Wu T L, Chen W P, Peng D L, Wu Z H, Ma M, Zheng Q S. The anomalous effect of electric field on friction for microscale structural superlubric graphite/Au contact. *Natl Sci Rev* **11**(9): nwae019 (2024)
[48] Jiang Y, Li Y, Liang B, Yang X F, Han T W, Wang Z. Tribological behavior of a charged atomic force microscope tip on graphene oxide films. *Nanotechnology* **23**(49): 495703 (2012)

Fu Wang received his Ph.D. degree from Lanzhou Institute of Chemical Physics, Chinese Academy of Sciences (CAS), in 2017. He is currently an associate professor at the State Key Laboratory of Solid Lubrication, Lanzhou Institute of Chemical Physics, CAS. His research focused on the applications and damage behavior of protective coatings in harsh environments.

Guang'an Zhang received his Ph.D. degree from Lanzhou University in 2006. He is currently a profesor at the State Key Laboratory of Solid Lubrication, Lanzhou Institute of Chemical Physics, Chinese Academy of Sciences, and serves as a member of the Surface Engineering Branch of the China Mechanical Engineering Society. His research interests include the promotion and application of PVD and PECVD technology to key mechanical moving parts, and he has successfully developed a series of solid lubrication coatings, such as diamond-like carbon, molybdenum disulfide, and metal nitride coatings.